

Liquid–Liquid Domain Miscibility Driven by Composition and Domain Thickness Mismatch in Ternary Lipid Monolayers

Maria Laura Fanani* and Bruno Maggio

Departamento de Química Biológica, Centro de Investigaciones en Química Biológica de Córdoba (CIQUIBIC), Facultad de Ciencias Químicas, CONICET, Universidad Nacional de Córdoba, Haya de la Torre y Medina Allende, Ciudad Universitaria, X5000HUA, Córdoba, Argentina

Received: August 4, 2010; Revised Manuscript Received: November 1, 2010

This work describes how changes in surface pressure modulate the molecular organization of Langmuir monolayers formed by ternary mixtures of dIPC/pSM/Dchol that exhibit coexistence of liquid-expanded (LE) and liquid-ordered (Lo) phases. It provides a theoretical framework for understanding the pressure-induced critical miscibility point characteristic of monolayer systems with liquid–liquid phase coexistence. From compression isotherms and Brewster angle microscopy of Langmuir monolayers with a composition close to a tie line, we determined experimental values of mean molecular areas, surface potential, and monolayer thickness and could estimate the mean molecular area and composition of each coexisting phase. A surface-pressure-induced enrichment of the PC component in the Lo phase reduces both the compositional miscibility gap and the hydrophobic mismatch between phases. The liquid–liquid miscibility transition point observed at ≈ 25 mN/m can be explained by a competition between thermal energy and the line tension arising from the hydrophobic mismatch between the coexisting liquid phases.

Introduction

In the 1980s, the characterization of a new lipid phase with intermediate properties between the gel and fluid phases, the liquid-ordered (Lo) phase, directed attention to cholesterol-rich membranes.^{1,2} These membranes showed liquid–liquid phase coexistence, interpreted as a consequence of formation of phospholipid–cholesterol complexes.^{3,4} Among the phospholipid species that interact with cholesterol, sphingomyelin emerged as an important partner for Lo phase formation in ternary mixtures that are often related to the “raft” concept in biomembranes.^{5,6} The ternary mixture of an expanded and condensed phospholipid (including sphingomyelin) and cholesterol (or its derivatives) became one of the most appealing lipid mixtures to study physical and biological properties of membranes exhibiting liquid–liquid phase coexistence.^{5,7,8}

In 2003, Prieto’s group reported a complete phase diagram for the ternary mixture of palmitoyloleoylIPC/pSM/Chol from fluorescence studies of multilamellar vesicles⁵ that closely correlated with fluorescence microscopy studies performed in giant unilamellar vesicles of identical composition.⁹ Even though a large amount of information on the composition and dynamics of Lo domains was obtained from bilayer studies, underlying molecular properties such as the mean molecular areas (MMA), the surface (dipole) potential contributions, and other supramolecular properties such as compressibility and compositional dependence of the segregated phase domains with the surface pressure are directly accessible only from monolayer experiments. PC/SM/Chol monolayers were previously studied by Slotte’s group¹⁰ showing a preferential interaction of Chol with SM. In the latter study, Lo domains were visualized at very low surface pressures and the miscibility transition pressures (the minimal pressure at which only one phase is present) was found below 7 mN/m.

Based on the ternary bulk phase diagram and the tie lines reported for PC/SM/Chol bilayers,^{5,11} in this work we studied the molecular properties and composition of the coexisting liquid phases using dIPC/pSM/Dchol monolayers along a tie line that includes the mixture with a molar ratio 1:1:1. The latter system represents a useful model for studying the properties of membranes containing cholesterol-enriched (Lo) domains.⁵ Since Lo domains occurring in cell membranes (usually referred to as “rafts”) are assumed to mediate important cell functions¹² (but see refs 13 and 14), the PC/SM/Chol ternary mixture has been named “the lipid raft mixture”^{5,15,16} and became profusely used for studying putative raft-related properties in artificial systems. The analysis of monolayers with a composition that corresponds to a tie line provides the thermodynamic base for considering that the properties of each coexisting phase are kept constant along such ternary compositional axis. Thus, the molecular packing and dipole properties of the monolayers that correspond to the extremes of (or any point along) the tie line can be analyzed and the physical properties and composition of each coexisting phase along the whole compositional axis can be deduced.

The combination of monolayer compression isotherms and BAM exploration provides detailed information on the molecular properties of each coexisting phase such as compressibility and thickness, as well as their dependence with the surface pressure, and allows calculation of their composition. Our results support that the Lo phase undergoes enrichment in the PC component as the surface pressure increases, with concomitant lowering of the domain thickness, while the liquid-expanded (LE) phase coexisting with the former diminishes in extent and remains rather invariant in lipid composition with the raise of surface pressure. A liquid–liquid miscibility transition pressure that behaves like a critical point, at which a single phase with intermediate characteristics occurs, is observed at ≈ 25 mN/m. This pressure is higher than the value reported previously for a similar ternary mixture but having different proportions of the

* Corresponding author. Tel.: +54-351-4334168. Fax: +54-351-4334074. E-mail: lfanani@fcq.unc.edu.ar.

components.¹⁰ By applying the theoretical model developed by Cohen et al.,¹⁷ the line tension between the coexisting phases and the minimum hydrophobic mismatch that can oppose thermal energy in order to allow for a stable interfacial line could be estimated.

Experimental Methods

Chemicals. Lipids (pSM, dIPC, and Dchol) over 99% pure by thin-layer chromatography were purchased from Avanti Polar Lipids (Alabaster, AL) and used without further purification. The cholesterol analogue Dchol was used instead of cholesterol because it minimizes air oxidation during experiments and shows interfacial behavior and phase diagram indistinguishable from that of cholesterol.^{3,18,19} Solvents and chemicals were of the highest commercial purity available. The water was purified by a Milli-Q (Millipore, Billerica, MA) system to yield a product with a resistivity of ~ 18.5 M Ω /cm. Absence of surface-active impurities was routinely checked as described elsewhere.²⁰ The lipid stock solution was kept under N₂ at -70 °C until use.

Monolayer Isotherms. Compression–expansion isotherms were obtained for pure or mixed lipid monolayers at different surface pressures. Typically, lipid monolayers were spread from 20 μ L of chloroform/methanol (2:1) solution onto a 266 cm² Teflon trough filled with 200 mL of 145 mM NaCl, pH ~ 5.6 . The film was relaxed for 5 min at 0 mN/m and subsequently compressed to the target pressure. Surface pressure and film area were continuously measured and recorded with a KSV Minitrough equipment (KSV, Helsinki, Finland) enclosed in an acrylic box. Compressibility modulus (C_s^{-1}) was calculated from the isotherm data as $C_s^{-1} = -A(d\pi/dA)_T$.^{21,22} All measurements were performed at a compression rate of 0.5–1 and 2–3 $\text{\AA}^2/\text{molecule}/\text{min}$ for condensed or expanded films, respectively. Two-fold reduction of the compression rate had no effect on the surface behavior.

BAM Measurements. Monolayers were prepared as described above but using a conveniently small Model 102 M equipment (NIMA Technology Ltd., Coventry, England) mounted on the stage of a Nanofilm EP3 Imaging Elipsometer (Accurion, Goettingen, Germany) used in the Brewster angle microscopy (BAM) mode. Zero reflection was set with a polarized 532 nm laser incident on the bare aqueous surface at the experimentally calibrated Brewster angle ($\approx 53.1^\circ$). After monolayer formation and compression, the reflected light was collected with a 20 \times objective and the reflectivity was calculated [typically $R = (\text{gray level} - 13.3) \times 10^{-7}$; calibration factors were checked for each individual experiment according to the manufacturer]. Assuming a refractive index of 1.33 and 1.49 for the aqueous surface and the lipid film respectively, R is related to the thickness (d) of the monolayer as follows: $R = 0.07784(-3.1684 \times 10^{-3} \times d)^{2,23}$

Estimation of Mean Molecular Areas (MMA) of Coexisting Phases. From experimental data of MMA of the monolayers exhibiting liquid–liquid phase coexistence (Figure 1), and from the proportion of area occupied by each phase (Figure 4a), the MMA for each coexisting phase can be calculated assuming that they belong to the same tie line. The validity of this assumption is further discussed later.

If we consider two lipid films showing liquid–liquid phase coexistence of different total compositions (I and II) but belonging to the same tie line, then

$$\frac{f_{LE}^{\text{II}}}{f_{LE}^{\text{I}}} = \frac{n_{LE}^{\text{II}}}{n_{LE}^{\text{I}}} \quad (1)$$

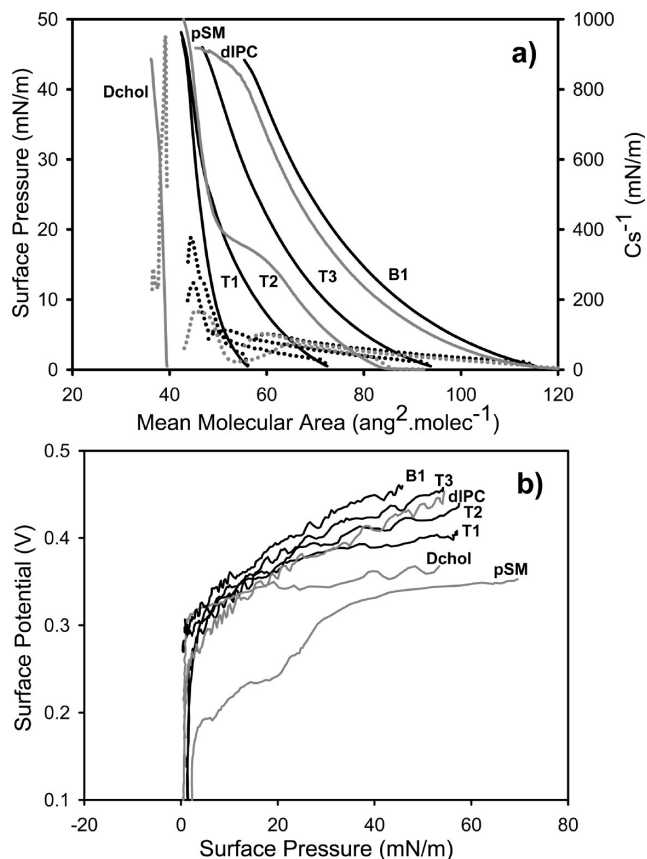


Figure 1. Surface behavior of ternary monolayers: (a) compression isotherm (full lines) and compressibility modulus (dotted lines), and (b) surface potential of lipid mixtures of dIPC/pSM/Dchol along the tie line (see text). Black lines correspond to mixed monolayers: ternary mixtures of dIPC/pSM/Dchol at (15:37:48) (T1), (34:33:33) (T2), and (60:26:14) (T3); and the binary mixture dIPC/pSM (80:20) (B1). For comparison, isotherms of pure lipid components are shown in gray lines. The figure shows representative curves from a set of three independent experiments.

where f_{LE}^{I} and f_{LE}^{II} are the area fraction occupied by the LE phase and n_{LE}^{I} and n_{LE}^{II} are the number of molecules in the LE phase in the total area analyzed (a'). The superscripts/subscripts I and II denote that the parameters are related to a monolayer of composition I and II, respectively. Additionally

$$n_{LE}^{\text{I}} = a' \bar{A}_I - n_{Lo}^{\text{I}} \quad (2)$$

where n_{Lo}^{I} is the number of lipid molecules in the Lo phase in a monolayer of area a' and \bar{A}_I is the MMA of the monolayer of composition I obtained experimentally. Note that a similar relation to eq 2 is also valid for the monolayer of composition II. Therefore, from eqs 1 and 2 we can deduce that

$$\frac{f_{LE}^{\text{II}}}{f_{LE}^{\text{I}}} = \frac{a' \bar{A}_{\text{II}} - n_{Lo}^{\text{II}}}{a' \bar{A}_{\text{I}} - n_{Lo}^{\text{I}}} \quad (3)$$

Reordering eq 3 and introducing

$$\frac{n_{Lo}^{\text{II}}}{n_{Lo}^{\text{I}}} = \frac{f_{Lo}^{\text{II}}}{f_{Lo}^{\text{I}}} \quad (4)$$

and

$$n = a^t \bar{A} \quad (13)$$

$$fc_{LE}^I = 1 - fc_{Lo}^I \quad (5)$$

(where \bar{A} is the experimental MMA of the mixed film) and

we obtain

$$n_{LE} = a^t \bar{A} - n_{Lo} \quad (14)$$

$$n_{Lo}^I = \frac{a^t (fc_{LE}^{II}/\bar{A}_I - fc_{LE}^I/\bar{A}_{II})}{1 - fc_{Lo}^{II}/fc_{Lo}^I} \quad (6)$$

in eq 12 and reordering, we obtain

and applying eq 6 to

$$n_{Lo}^i = a^t \bar{A} (X^i - X_{LE}^i) + n_{Lo} X_{LE}^i \quad (15)$$

$$\bar{A}_{Lo} = \frac{fc_{Lo}^I a^t}{n_{Lo}^I} \quad (7)$$

Therefore, the mole fraction of the i component in the Lo phase is

we can obtain the MMA of the Lo phase as follows

$$X_{Lo}^i = \frac{a^t \bar{A} (X^i - X_{LE}^i) + n_{Lo} X_{LE}^i}{n_{Lo}} \quad (16)$$

$$\bar{A}_{Lo} = \frac{fc_{Lo}^I - fc_{Lo}^{II}}{fc_{LE}^{II}/\bar{A}_I - fc_{LE}^I/\bar{A}_{II}} \quad (8)$$

Note that this value of MMA is valid for the Lo phase of any monolayer with a composition that belongs to the analyzed tie line.

With the information above, the MMA of the LE phase can also be calculated. By equalizing

$$a^t = n_{Lo}^I \bar{A}_{Lo} + n_{LE}^I \bar{A}_{LE} \quad (9)$$

and

$$a^t = (n_{Lo}^I + n_{LE}^I) \bar{A}_I \quad (10)$$

and replacing n_{LE}^I by eq 2, we obtain the MMA of the LE phase of any monolayer whose composition belongs to the tie line as follows:

$$\bar{A}_{LE} = \frac{n_{Lo}^I (\bar{A}_I - \bar{A}_{Lo})}{a^t \bar{A}_I - n_{Lo}^I} + \bar{A}_I \quad (11)$$

Estimation of the Mole Fraction of Each Lipid Component in the Lo Phase. From experimental data on the composition of the LE phase (see Figure 4a and text) and the calculation of the number of molecules in the Lo phase for a given lipid film (n_{Lo}^I) as described by eq 6 (for further calculation we will use n_{Lo} since only a single lipid composition will be analyzed), the mole fraction of each component in the Lo phase can be estimated. The number of molecules i in the Lo phase is

$$n_{Lo}^i = n X^i - n_{LE} X_{LE}^i \quad (12)$$

where n and n_{LE} are the total number of molecules and the number of molecules in the LE phase, respectively, in the analyzed area (a^t), and X^i and X_{LE}^i are the total mole fraction and the mole fraction of the i component in the LE phase (experimental data, see Figure 4a and text), respectively. Replacing

Results

Compression Isotherms of Ternary Monolayers of dIPC/pSM/Dchol Show Smooth Behavior along the Compositional Axis. The ternary mixtures dIPC/pSM/Dchol (15:37:48), (34:33:33), and (60:26:14), and the binary mixture dIPC/pSM (80:20) will be named T1, T2, T3, and B1, respectively. These lipid mixtures were chosen by analogy to the phase diagram for PC/SM/Chol ternary mixture reported for bilayers^{5,11} where they are demonstrated to belong to the tie line that includes the 1:1:1 composition point. Thus, the ternary mixtures are expected to show LE–Lo phase coexistence, with both phases keeping their general properties along the compositional axis and only changing the relative proportion of each phase (the more Dchol content should result in more surface area covered by the Lo phase).

The surface pressure–mean molecular area (MMA) isotherms for the ternary monolayers T1, T2, and T3 with decreasing content of Dchol (and also of pSM) and the binary monolayer B1 are shown in Figure 1a. All the mixtures analyzed show a monotonic behavior and the phase transition that occurs at about 15–18 mN/m in pure pSM is not observed in the mixed films. The analysis of the compressibility modulus (C_s^{-1}) in Figure 1a shows that the mixed monolayer containing 48% Dchol (T1) is more condensed (C_s^{-1} values >100 mN/m²⁴) while the monolayers containing less than 33% Dchol and pSM (T3 and B1) show a liquid-expanded character (C_s^{-1} values <100 mN/m). After the initial rise at lift-off, the surface potential of the monolayers (Figure 1b) increases with the surface pressure and this is more pronounced for the expanded monolayers than for pure Dchol. The latter film shows molecular parameters having a weak dependency on the surface pressure (Figure 1). From the analysis of MMA as a function of composition (Figure 2), it can be seen that only ternary mixtures at low surface pressures and high Dchol content show condensation of the MMA with respect to an ideal mixture of identical composition (Figure 2a). Several studies have shown a condensed capacity of Chol (and also Dchol) when incorporated in binary and ternary mixtures with phospholipids.^{3,19,25,26} We will demonstrate further below that a condensing effect of Dchol is better observed when the Dchol-rich phase is analyzed separately. The surface potential normalized per molecular surface density (Figure 2b) also shows a rather smooth variation with the increase of Dchol + pSM.

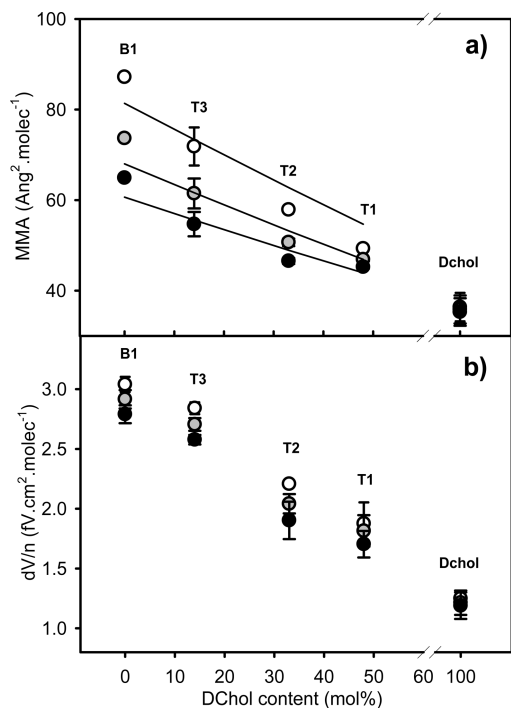


Figure 2. Mean molecular area (MMA) and surface potential per molecular surface density (dV/n) as a function of monolayer composition (T1, T2, T3, and B1 as detailed in the legend to Figure 1). Note that an increase in Dchol is concomitant with an increase in pSM content. Open, gray, and black circles represent measurements at 10, 20, and 30 mN/m, respectively. Full lines represent the MMA values calculated for an ideal ternary mixture. The values are average \pm SEM from a set of three independent experiments. When no error bar is observed, the corresponding SEM value is smaller than the size of the point.

Ternary Monolayers Show Coexistence of LE and Lo Phases Merging into a Single Phase at ~ 25 mN/m. Brewster angle microscopy (BAM) visualization of the ternary lipid films reveals phase coexistence in the ternary mixtures T1, T2, and T3 (Figure 3). A thick phase (light gray) forms circular domains immersed in a thinner phase (dark gray). In all the samples the domains become larger with an increase of the surface pressure. The area coverage by the light gray phase increases with the

proportion of Dchol + pSM (in the sequence $T3 < T2 < T1$) (Figures 3 and 4). Under all conditions studied, the Dchol-rich domains exhibit rounded boundaries that correspond to typical liquid–liquid immiscibility. This supports the assignment of a liquid-ordered (Lo) character to the thick Dchol-rich phase and a liquid-expanded (LE) character to the thinner continuous phase.

All three ternary mixtures analyzed clearly show liquid–liquid phase coexistence that remains stable at surface pressures up to 20 mN/m (see Figure 3). Over the pressure range of 24–26 mN/m the ternary monolayers exhibit instability of the domains and morphologies with undulated boundaries can be observed. These are more evident when the areas of Lo and LE phases are similar (see Figure 3, T2 at 25 mN/m and Figure S1 in the Supporting Information). These structures can exist for a few minutes until a single phase (with intermediate thickness) is established. This phenomenon represents a miscibility transition point with the characteristics of a system close to a critical pressure point,²⁷ in analogy to the phenomena described for bilayers of similar composition when the system is near a critical temperature.^{28,29} Specifically, miscibility transition points (not shown) are observed for T1 at 24.5 ± 1 mN/m, for T2 at 25 ± 1 mN/m, and for T3 at 26 ± 1 mN/m. The pressure necessary for achieving the critical point is higher in our system compared to that previously reported for PC/SM/Chol ternary monolayers with different lipid proportions (25 mN/m in ours, compared to less than 7 mN/m),¹⁰ and it is also higher than that reported for binary pSM/Dchol mixtures.²⁵ This difference may be due not only to variations of the chemical structure of the components (i.e., chain length, asymmetry) but also of their proportion in the mixture.²⁹ Higher critical pressures (in the 40 mN/m range) were only reported for ternary mixtures of Dchol with a long and a short acyl chain PC.²⁹

From the quantitative analysis of BAM images of ternary monolayers T1, T2, and T3 (as shown in Figure 3), the area occupied for each phase and the values of film thickness (d) assuming a constant refraction index for the lipid film of 1.49 (see Experimental Methods) can be estimated. Figure 4a shows that an increase of surface pressure induces an increase of the amount of the Lo phase, with a tendency to decrease its thickness (Figure 4b, upper points in shaded area). Concomi-

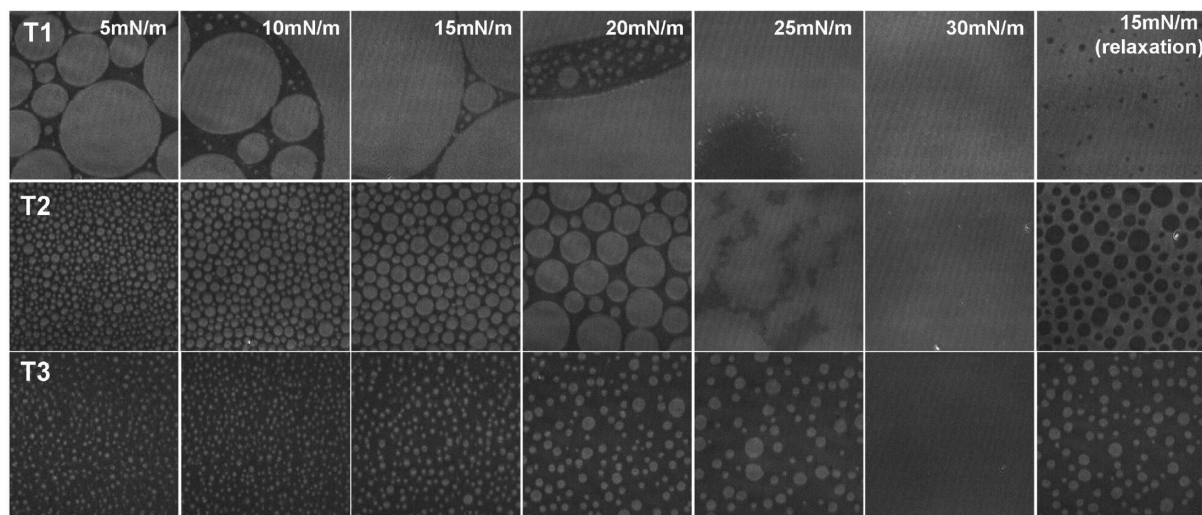


Figure 3. BAM visualization of ternary mixtures containing dIPC/pSM/Dchol (T1, T2, and T3, as detailed in the legend to Figure 1). Images were taken at the surface pressure given in each image column. For better visualization, the lower 0–70 gray level range (from the 0 to 255 original scale) was selected in order to keep the gray level–film thickness relationship. Images for T1 and T2 at 25 mN/m correspond to unstable morphologies, and the surface became homogeneous in a few minutes. Images are representative of two independent experiments. Image size is $150 \times 150 \mu\text{m}$.

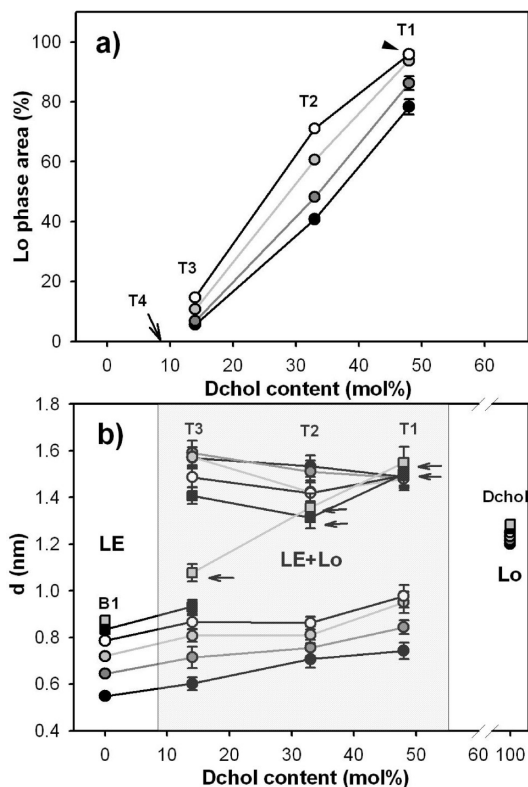


Figure 4. Quantitative analysis of the coexisting phases in mixed monolayers T1, T2, and T3. (a) The area occupied by the Dchol-rich (Lo) phase and (b) the film thickness of each phase are shown as a function of Dchol (and also of pSM) content at 5 mN/m (black circles), 10 mN/m (dark gray circles), 15 mN/m (light gray circles), and 20 mN/m (white circles) for both panels and at 25 mN/m (black square) and 30 mN/m (gray square) for panel b only. Arrow in panel a indicates the calculated composition of the ternary monolayer that exhibiting LE phase only (T4). Arrow head in panel a highlights a condition where the monolayer does not behave as belonging to the same tie line (see text). The shaded area in panel b highlights the data for the ternary monolayers T1, T2, and T3. Monolayers analyzed at 0% (B1) and 100% of Dchol content in panel b show a single homogeneous phase. Arrows indicate measurement in single-phase ternary monolayers, above the critical pressure. The values are average \pm SEM from a set of 12 images/surface pressure analyzed in two independent experiments.

tantly, we observed an increase of the thickness of the continuous LE phase. The thickness of both coexisting phases shows values that are rather independent of the total film composition. Above the miscibility transition point the thickness of the resultant single phase depends markedly on the total monolayer composition (Figure 4b, see arrows).

Estimation of the Composition of the LE Phase in Ternary Monolayers. The analysis of the area coverage by the Lo phase shown in Figure 4a for the mixed monolayers T1, T2, and T3 indicates an essentially linear dependency of the extent of the Lo phase with the Dchol content (and also with the pSM content, not shown). The only exception is observed in conditions where the LE phase occupies less than 5% of the total area (see arrowhead in Figure 4a). This can be explained as follows: an increase of surface pressure involves redistribution of lipid between phases (dIPC moves from the LE to the Lo); this will be demonstrated further below. Such redistribution needs a certain amount of LE phase available (>5 area %) from which dIPC could be acquired; thus, the mixed monolayer T1 at high surface pressure (arrowhead in Figure 4a) does not have enough LE phase, with the available dIPC, to be incorporated in the Lo phase and the resultant phase composition falls off the tie line.

The data in Figure 4a was used to calculate the composition of a monolayer where the amount of area coverage by the Lo phase is null. The lines corresponding to different surface pressures converge to the same value (see arrow in Figure 4a), within an error of less than 2%. This value corresponds to a content of Dchol in the LE phase of 9.4 ± 0.2 mol % and of pSM of 24.5 ± 0.1 mol %. Therefore, for further calculations the composition of the LE phase (in coexistence with the Lo phase) was taken as dIPC/pSM/Dchol (66.1:24.5:9.4) and will be referred to as T4.

The general linear variation of the phase areas with the composition axis (Figure 4a) supports data available in the literature that assigns to a tie line the PC/SM/Chol system in the proportions used herein.⁵ Along the tie line, supramolecular properties such as composition, MMA, compressibility, etc. of each phase ought to be conserved along the compositional axis and only the extent of each phase should change. Thus, a behavior corresponding to such tie line for the mixed monolayers T1, T2, and T3 will be considered for further analysis, with the mixed monolayer T4 taken as the dIPC-enriched limit of the tie line where a 100% LE phase (no Lo phase) occurs.

Estimation of Mean Molecular Areas of Coexisting LE and Lo Phases in Ternary Monolayers. From the experimental data of MMA of the ternary monolayers showing liquid–liquid phase coexistence T1, T2, and T3 (Figure 1) and from the proportion of area occupied by each phase in the same mixed monolayers (Figure 4a), the MMA for each coexisting phase (MMA_{LE} and MMA_{Lo}) considering that they belong to the same tie line can be calculated as detailed in the Experimental Methods section. Equations 8 and 11 were used in pairs for the three ternary monolayers T1, T2, and T3 (three possible combinations). The resultant value of MMA calculated at each surface pressure has an SEM of less than 1%. Figure 5a (open circles) shows the calculated MMA_{LE} at different surface pressures. The MMA_{LE} values diminish with an increase of surface pressure, in a manner characteristic of a LE phase. This change is usually interpreted as a smooth reorientation of the molecules under compression to a position where the hydrocarbon chains become more perpendicular to the interface. From these data we can calculate a compressibility modulus for the LE phase that results, as expected, in values corresponding to a lipid-expanded phase ($C_s^{-1} = 80 \pm 1$ mN/m at a surface pressure of 20 mN/m). The calculated MMA_{LE} (from eq 11, Figure 5a open circles) shows full coincidence with an ideal MMA of a monolayer of composition T4 (MMA_{T4}) (full line in Figure 5a) that corresponds to the LE end of the studied tie line. This result is again in keeping with the ternary mixtures studied having compositions that correspond to a tie line. For the calculation of MMA_{T4} , the MMA values of pSM were taken as being in the LE state (see dotted line in Figure 5b). The close coincidence of the calculated MMA_{LE} and MMA_{T4} indicates that the molecules in the LE phase show an ideal behavior, with the capacity of keeping the pSM component in a LE state even at surface pressures where, in the pure state, it should be present as liquid condensed (Figure 5b). The use of experimental data in eq 8 provides the calculated value of MMA_{Lo} at each surface pressure analyzed (Figure 5a, closed circles).

Composition of the Lo Phase in Ternary Monolayers Is Dependent on Surface Pressure. Based on the calculation of the number of molecules present in the Lo phase for each ternary mixture (eq 6) and the estimated composition of the LE phase (mixed monolayer T4), the composition of the Lo phase can be calculated as described in the Experimental Methods section (eq 16) for the three ternary mixtures T1, T2, and T3. The results

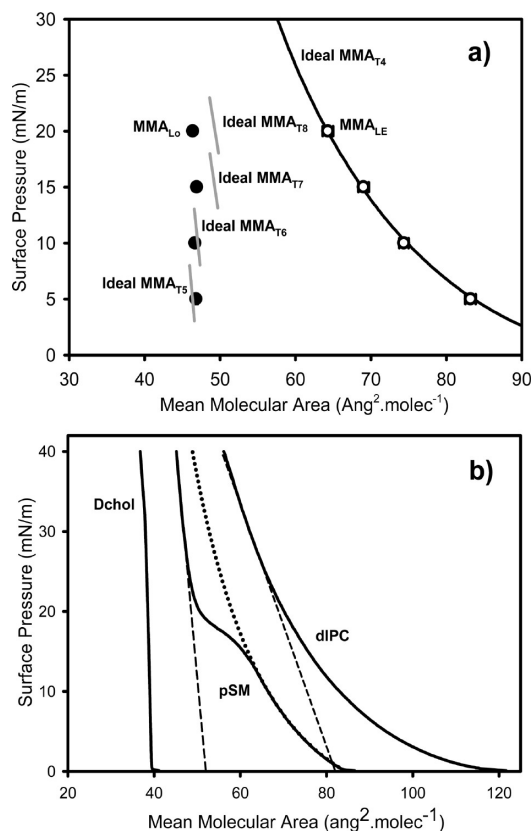


Figure 5. Calculated mean molecular areas (MMA) for the coexisting phases in ternary mixtures. (a) Open circles show the MMA of the LE phase calculated as detailed in Experimental Methods (eq 11). The black full line represents the ideal MMA for the T4 mixed monolayer (dIPC/pSM/Dchol (66.1:24.5:9.4), see text) assuming that the pSM component remains in the LE state (as shown in panel b, dotted line). Closed circles represent the calculated MMA of the Lo phase as detailed in Experimental Methods (eq 8). The gray vertical line segments represent the ideal MMA for the ternary monolayers T5, T6, T7, and T8 as calculated from eq 16 at 5, 10, 15, and 20 mN/m, respectively (see text). For simplicity, only the segments of the isotherms in the range of the surface pressure at which these compositions were calculated were plotted. The gray line segments were calculated from the MMA of the pure component monolayers assuming that the pSM and dIPC components are in the condensed state (as shown in panel b, dashed lines). When no error bar is observed, the corresponding SEM value is smaller than the size of the point. (b) Compression isotherms are shown for the pure components Dchol, pSM, and dIPC (full lines) and calculated curves for pSM, as if it was in an expanded state along the whole surface pressure range (dotted line, by fitting with an inverse second order polynomial equation). The dashed lines show calculated curves for pSM and dIPC as if they were in a condensed state (by fitting with a linear equation).

show that the composition of the Lo phase in these mixtures is dependent on the surface pressure (Figure 6a). The resultant compositions are dIPC/pSM/Dchol (6:40:54) at 5 mN/m, (10:39:51) at 10 mN/m, (20:36:44) at 15 mN/m, and (24:35:41) at 20 mN/m; and they will be referred to as T5, T6, T7, and T8, respectively. From the information in Figure 6a, a surface pressure–composition phase diagram along the proportions of each component can be drawn (Figure 6b–d). Figure 6 indicates that the Lo phase becomes enriched in the PC component and concomitantly diluted in the Dchol and pSM content with an increase of surface pressure, while the composition of the LE phase remains approximately constant at all surface pressures (Figure 6b–d).

With the aim of further understanding the properties of the Lo phase of ternary monolayers, we also calculated the ideal

MMA of the ternary mixtures T5 to T8 (shown in Figure 6) and plotted them as gray line segments in Figure 5b. These MMA values correspond to the composition of the Lo phase of mixed monolayers T1, T2, and T3 (and the Dchol end of the tie line) at different surface pressures. For this calculation, the MMA of pure components were used, weighted by the proportion of each component in the mixture. A better fitting with the MMA_{Lo} calculated in the previous section was obtained when the lipid component pSM was taken as being in the liquid condensed phase and dIPC as behaving with the same character than in a monolayer at 25–35 mN/m (as shown by the dashed lines in Figure 5b). Thus, Figure 5a allows comparison of the calculated MMA of the Lo phase obtained in two different manners: the closed circles are the result of applying eq 8 (MMA_{Lo}) to the experimental data obtained for the phase extent and MMA of the ternary mixture (data from Figures 1 and 4) and the vertical gray line segments show the results of the calculation of an ideal MMA of the Lo phase according to eq 16 (ideal MMA_{T5} , MMA_{T6} , MMA_{T7} , and MMA_{T8}). The results indicate that the molecules in the Lo phase undergo a condensation that is larger than that occurring as a consequence of a simple phase transition effect, indirectly supporting the hypothesis of the formation of complexes in cholesterol–phospholipid interactions.³

Alltogether, the effect of surface pressure on a ternary mixture that exhibits liquid–liquid phase coexistence shows reordering (to a structure more perpendicular to the interface) of the molecules present in the LE phase, with a decrease of the amount of phase (and also of the MMA) and an increase of the LE phase thickness, with a rather constant phase composition (Figure 6). On the other hand, the Lo phase shows a condensed character and bears enrichment in dIPC induced by pressure (Figure 6). Concomitantly, the thickness of the Lo phase decreases with the incorporation of the short-chain lipid. As a result, an increase of surface pressure induces a reduction of the thickness mismatch between phases, reaching a minimum thickness gap (Figure 7a) before the linear interface (domain boundary) becomes unstable and vanishes, forming a single phase.

Line Tension of Domain Boundary as a Determinant Factor for Lo Domain Shape. Liquid domain shape is controlled by the counteracting forces of internal dipole repulsion within the domain and line tension.³⁰ The ternary mixed monolayers studied in this work show circular Lo domains surrounded by a LE continuous phase. By a closer examination of Figure 1b, we observed that our measurements of surface potential show almost superimposed values for the ternary films at surface pressures below 25 mN/m. This means that, even when all three ternary mixtures studied exhibit a large difference in the Lo/LE area relationship (Figures 3 and 4a), the surface potentials of the whole monolayers remain with an essentially similar value (≈ 0.37 V at 20 mN/m, Figure 1b) even if the molecular density (MMA^{-1}) change (see Figure 2a). This leads to the conclusion that both coexisting liquid phases have similar resultant dipolar properties. Thus, if both phases show similar overall dipolar properties, dipole repulsion should not be a determinant for domain shape and interdomain structuring in this case. This conclusion is supported by the observation of rounded domains in all samples, indicating that line tension prevails.

Hydrophobic Mismatch between Coexisting LE and Lo Phases Can Account for the Domain Boundary Line Tension. The concept known as hydrophobic mismatch originated from considering that, when the lengths of the membrane spanning domains of membrane proteins are different from the

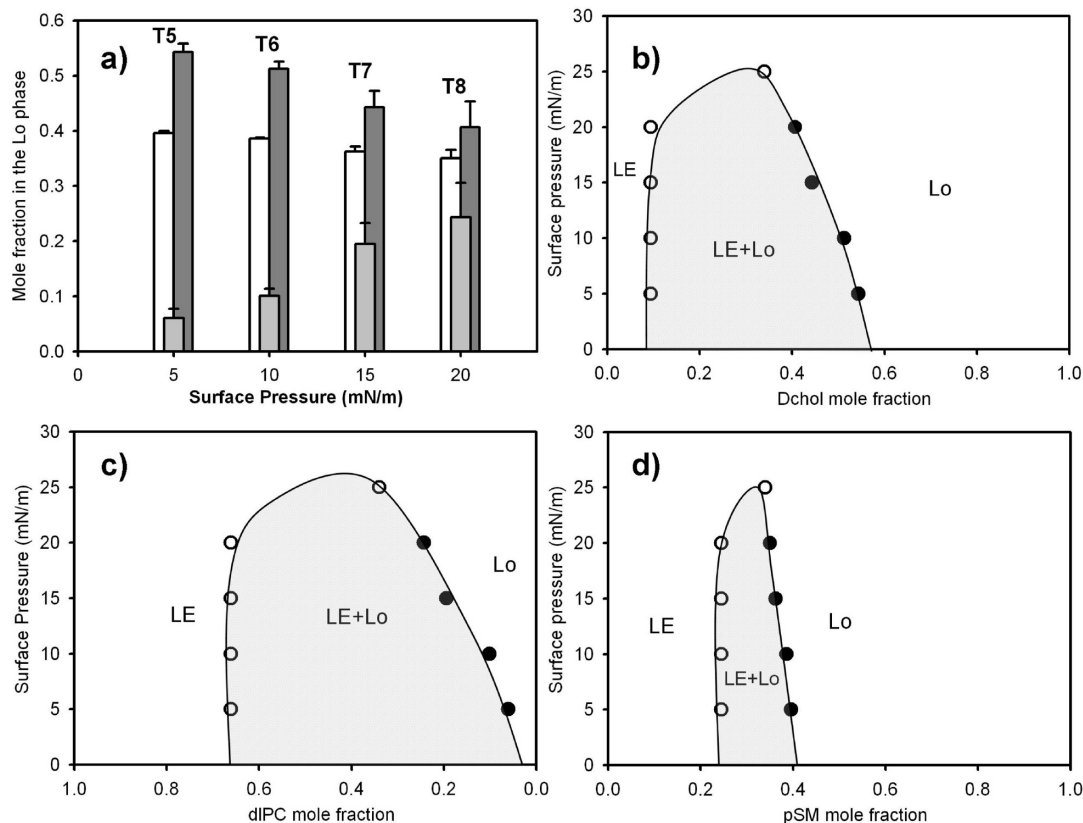


Figure 6. Dependence of the Lo and LE phases composition on the surface pressure. (a) Mole fraction of the lipid components in the ternary monolayers T5, T6, T7, and T8 corresponding to the Lo phase in ternary monolayers T1, T2, and T3 as a function of surface pressure (as calculated from eq 16): pSM (white bars), dIPC (light gray bars), and Dchol (dark gray bars). Error bars represent SEM. (b–d) Surface pressure–composition phase diagram for the dIPC/pSM/Dchol (T2) ternary mixture along the Dchol (b), dIPC (c), or pSM (d) compositional axis.

thickness of the surrounding lipid bilayer, a significant hydrophobic surface would be exposed to water. It is largely known that lipid deformations are necessary to compensate this mismatch and minimize energetic costs.^{31,32} In membranes where coexistence of phases with different thickness occurs, a similar “hydrophobic mismatch” phenomena could be considered.³³ From our measurement of the phase thickness, the hydrophobic mismatch between phases can be calculated directly. Figure 7a shows that the hydrophobic mismatch between phases diminishes with an increase of surface pressure, to a limit of ≈ 0.47 nm. Beyond that surface pressure limit, the line between domains becomes unstable, the LE and Lo phases merge, and the monolayer exhibits a single homogeneous surface phase. In recent years, a theoretical model that approaches membrane hydrophobic mismatch phenomena was developed by Cohen et. al¹⁷ considering that, different from the membrane protein-surrounding bilayer system, where only the surround can deform in response to the mismatch, both lipid phases may deform in membranes. Taking into account this theoretical model, the energy per unit length of boundary, namely line tension (γ), can be calculated from our data of phase thickness as follows:

$$\gamma = \frac{\sqrt{B_{LE}K_{LE}B_{Lo}K_{Lo}}}{\sqrt{B_{Lo}K_{Lo}} + \sqrt{B_{LE}K_{LE}h_o^2}} \delta^2 - \frac{1}{2} \frac{(J_{LE}B_{LE} - J_{Lo}B_{Lo})^2}{\sqrt{B_{Lo}K_{Lo}} + \sqrt{B_{LE}K_{LE}}} \quad (17)$$

δ is the phase thickness mismatch, h_o is the average height of the two phases Lo and LE: $h_o = (h_{Lo} + h_{LE})/2$ where h is the monolayer thickness; B is the elastic splay modulus; K is the tilt modulus; and J is the spontaneous curvature of the mono-

layer. For this calculation, monolayer deformation parameters values for both phases Lo and LE were assumed as $B_{Lo} = B_{LE} = 10kT$, and $K_{Lo} = K_{LE} = 40$ mN/m and $J_{Lo} = J_{LE} = 0$ for a soft domain.¹⁷ Figure 7b shows the calculated line tension values as a function of the surface pressure for all three ternary mixtures T1, T2, and T3. The line tension decreases with an increase of surface pressure, in agreement with previous pioneering work by McConnell.³⁴ In the latter work, a linear decrease of the line tension with pressure from 1.6 to 0.1 pN was reported for dimyristoylPC/Chol mixed monolayers. Our results indicate a minimum line tension for maintaining a stable domain border of ≈ 3.3 pN (corresponding to a minimum hydrophobic mismatch of ≈ 0.47 nm) before the occurrence of line disruption and phase merging. As is intuitive, and also observed for systems that reach a critical temperature by heating,²⁸ the critical pressure should correspond to a nearly null line tension. In our system, and using Cohen’s theoretical model, we could calculate a minimum value of line tension that is higher than the minimum value (about 0.1 pN) reported in other systems near critical points.^{28,35} This may indicate either that in Cohen’s model some factors contributing to line tension are not included or that there may be a counteracting force favoring phase mixing that destabilizes the line boundary when its energy is less than 3.3 pN.

Miscibility Transition Pressure Is Reached When the Line Tension Energy Acquires Thermal Energy Levels. In order to consider thermal energy, we calculated the number of molecules in two rows at each side of the domain boundary.¹⁷ Values of 60.5 and 46.1 $\text{\AA}^2/\text{molecule}$ for sectional molecular area in the LE and Lo phases, respectively (see MMA values in Figure 5a), were used as to estimate molecular diameters.

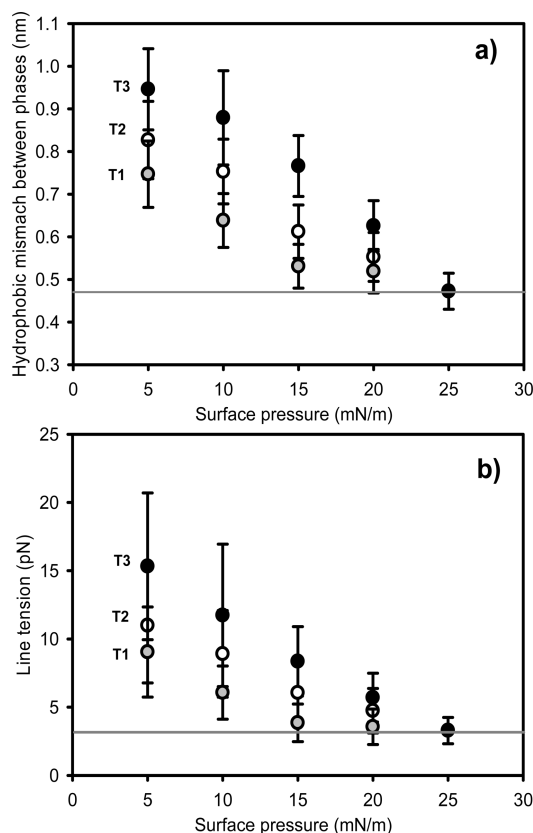


Figure 7. Phase height gap and line tension in ternary monolayers showing liquid–liquid phase coexistence. Hydrophobic mismatch between coexisting liquid phases (a) and line tension (b) as a function of surface pressure. Film composition: T1 (gray circles), T2 (open circles), and T3 (close circles) (see details in the legend to Figure 1). Line tension was calculated from the model in¹⁷ assuming a soft domain, with $B_{Lo} = B_{LE} = 10kT$, and $k_{Lo} = k_{LE} = 40$ mN/m, spontaneous curvature $J_{Lo} = J_{LE} = 0$. Error bars are SEM. The horizontal lines represent the minimum height gap and line tension that support a stable lateral interface, as deduced from the microscopy images.

The calculated thermal energy of the four rows of molecules on the interfacial line of a domain of $50 \mu\text{m}$ at 22°C results in a value of ≈ 3 fJ. The difference between this calculated thermal energy with the line tension of a domain of the same diameter (≈ 0.5 fJ) is less than 1 order of magnitude. This comparison suggests that, according to Cohen's model of interfacial boundary, and considering our assumption of a constant reflection index for both phases in our BAM measurements of the domain thickness, the minimum hydrophobic mismatch of 0.47 nm corresponds to a line tension that is very close to the thermal energy of the interfacial system, thus justifying its vanishing, the domain instability, and consequent phase merging.

Discussion

In the present work, we studied a series of ternary monolayers where the contents of all three components were varied simultaneously in order to be kept on a phase coexistence tie line. Previous work by Slotte's group explored binary monolayers of PC/Chol and SM/Chol³⁶ and ternary PC/SM/Chol monolayers¹⁰ by keeping a constant Chol content and progressively replacing the PC component by SM. The latter work described liquid–liquid coexistence in the ternary monolayers up to a relatively low surface pressure at which the components became miscible. In that system the coexisting Lo and LE phases observed should suffer changes of composition in all three

components along the compositional axis because the mixture does not belong to a tie line. Thus, each compositional point behaves as an independent case and the comparison with other ternary mixtures is not straightforward. In our approach, ternary mixtures that belong to the same tie line are studied and the information obtained from one ternary monolayer brings about information that is also valid for other proportions of the same lipids in the ternary system. By comparison of the variation of the extent of the Lo phase along the compositional axis, we could estimate molecular parameters that describe the physical properties of the average molecule in each coexisting phase. From the analysis of MMA, we show that the LE phase exhibits an ideal behavior, having the capacity of keeping pSM in an expanded state at high surface pressures; the Lo phase has a condensation capacity keeping pSM and dlPC in a condensed state even at low surface pressures (see Figure 5). Therefore, the characteristic phase transition of pure pSM is abolished (see Figure 1). We were also able to calculate the composition of the coexisting phases as a function of surface pressure. As far as we know, this is the first study that reports the change of composition of a ternary two-phase lipid system as a function of the surface pressure. The results support a surface pressure-dependent incorporation of the short chain PC in the Lo phase. This leads to a reduction of the compositional gap and also of the hydrophobic length mismatch between the phases which causes destabilization of the domain boundary and subsequent merging.

As mentioned in the Introduction, the miscibility critical pressure phenomenon was first described by McConnell in binary monolayers composed of Dchol/phospholipid³⁰ and later in ternary Dchol/phospholipid1 (P1)/phospholipid2 (P2) systems.²⁹ The latter study evidenced the tendency to exhibit higher miscibility transition pressures when P1 and P2 are phospholipids with an acyl chain difference of four to eight methylene groups or when double-saturated and double-unsaturated phospholipids were combined. This finding was interpreted on the basis of favorable/unfavorable phospholipid interactions. From our results, the acyl chain length difference or saturation/unsaturation of the phospholipids P1 and P2 may also modulate the thickness of the Lo and LE phases depending on their partition tendency and hydrophobic mismatch.

The boundary line tension of Lo domains has been previously calculated for different lipid systems by several methods. In an early work, McConnell et al³⁴ reported values of line tension for a monolayer reaching the critical pressure 1 order of magnitude lower than the values reported here. In a subsequent work,³⁷ it was shown that those low values could be a consequence of neglecting the monolayer viscosity in the former calculation. A correction of that parameter led to line tension values of 7.5 pN for the gas–LE interface, well in the range of the values reported in the present work. Line tension values for PC/SM/Chol bilayers were also previously reported.³⁸ In the latter work, line tension values 4-fold lower than those calculated in our work were found for a bilayer showing similar hydrophobic mismatch (0.8 pN for a mismatch of 0.67 nm), using the same theoretical model. A major source of variation can be the estimation of monolayer thickness. In ref 38, the bilayer thickness (5.5 nm) was taken from AFM measurements of fully hydrated dipalmitoylIPC bilayers at room temperature (gel phase state). Such estimation should result in higher monolayer thickness values because the dipalmitoylIPC gel phase is thicker than the Lo or LE phase. Additionally, the thickness estimated by AFM includes the hydration water and polar head group layer. In the present work, we measured monolayer thickness

from BAM images. This technique is sensitive to the presence of a film surface with a reflectivity index different to that of the subphase. The polar head group region of lipids is highly hydrated, and its reflectivity index is close to that of water. Thus, in practice, BAM measures mostly the hydrophobic region of the film. Since the theoretical model used for calculation of line tension includes only the hydrophobic properties of the membrane we consider our measurements of monolayer thickness quite adequate.

From Figure 7b we found that a line tension of at least ≈ 3.3 pN is necessary to counteract thermal energy which favors line tension vanishing and phase homogeneity, a fact that occurs at surface pressures of 24–26 mN/m in our system. A considerable amount of experimental evidence shows the presence of liquid–liquid phase coexistence in bilayers composed of PC/SM/Chol in similar proportions and temperatures to those used in our work.^{5,11,38,39} Since the bilayer membrane is considered to bear an average surface pressure in the range of 30–35 mN/m,⁴⁰ why should we observe liquid–liquid phase coexistence only at surface pressures below 26 mN/m? This apparent bilayer/monolayer difference may be a consequence of domain coupling between both hemilayers of the bilayer. The coupling of domain boundaries in two hemilayers should result in the sum of the line tension of each, thus stabilizing the line interface. This may confer stability to Lo domains at higher surface pressures in bilayers even when less hydrophobic mismatch in each monolayer occurs. This interpretation has been analyzed recently through molecular simulation.⁴¹

In summary, with experimental compression isotherms and BAM observations of ternary mixtures along a compositional tie line over which LE and Lo phase coexist, together with the use of Cohen's model of interfacial line tension,¹⁷ we could simultaneously relate compositional change of the Lo phase with the line tension of domain boundaries as a function of surface pressure. The enrichment of the Lo phase in the short component dIPC results in a decrease of line tension (driven primarily by a decrease of hydrophobic mismatch between phases) that is finally overcome by the thermal energy of the interfacial system. In this manner, the liquid–liquid miscibility transition that results from monolayer compression can be explained.

Abbreviations. SM, sphingomyelin, pSM, *N*-palmitoylsphingomyelin; Chol, cholesterol; Dchol, dihydrocholesterol; PC, phosphatidylcholine; dIPC, dilauroylphosphatidylcholine; LE, liquid-expanded; Lo, liquid-ordered; BAM; Brewster angle microscopy; MMA, mean molecular area; C_s^{-1} , compressibility modulus.

Acknowledgment. This work was supported by SECyT-UNC, ACC-MinCyT (Prov. Córdoba), CONICET and FONCyT (Argentina); some aspects of this investigation are inscribed within the PAE 22642 network in Nanobiosciences. B.M. and M.L.F. are Career Investigators of CONICET.

Supporting Information Available: BAM visualization of ternary monolayers containing dIPC/pSM/Dchol (34:33:33) (T₂) at surface pressure in the 25–26 mN/m range. This material is available free of charge via the Internet at <http://pubs.acs.org>.

References and Notes

(1) Ipsen, J. H.; Karlstrom, G.; Mouritsen, O. G.; Wennerstrom, H.; Zuckermann, M. J. *Biochim. Biophys. Acta* **1987**, *905*, 162–172.

- (2) Mouritsen, O. G. *Biochim. Biophys. Acta* **2010**, *1798*, 1286–1288.
 (3) McConnell, H. M.; Radhakrishnan, A. *Biochim. Biophys. Acta* **2003**, *1610*, 159–73.
 (4) McConnell, H. M.; Vrljic, M. *Annu. Rev. Biophys. Biomol. Struct.* **2003**, *32*, 469–492.
 (5) de Almeida, R. F.; Fedorov, A.; Prieto, M. *Biophys. J.* **2003**, *85*, 2406–2416.
 (6) Ramstedt, B.; Slotte, J. P. *Biochim. Biophys. Acta* **2006**, *1758*, 1945–56.
 (7) Veatch, S. L.; Keller, S. L. *Biochim. Biophys. Acta* **2005**, *1746*, 172–185.
 (8) Marsh, D. *Biochim. Biophys. Acta* **2009**, *1788*, 2114–2123.
 (9) Veatch, S. L.; Keller, S. L. *Phys. Rev. Lett.* **2005**, *94*, 148101.
 (10) Mattjus, P.; Slotte, J. P. *Chem Phys Lipids* **1996**, *81*, 69–80.
 (11) Silva, L. C.; Futerman, A. H.; Prieto, M. *Biophys. J.* **2009**, *96*, 3210–3222.
 (12) Edidin, M. *Annu. Rev. Biophys. Biomol. Struct.* **2003**, *32*, 257–283.
 (13) Lichtenberg, D.; Goni, F. M.; Heerklotz, H. *Trends Biochem. Sci.* **2005**, *30*, 430–6.
 (14) McMullen, T. P. W.; Lewis, R. N.; McElhaney, R. N. *Curr. Opin. Colloid Interface Sci.* **2004**, *8*, 459–468.
 (15) Dietrich, C.; Bagatolli, L. A.; Volovyk, Z. N.; Thompson, N. L.; Levi, M.; Jacobson, K.; Gratton, E. *Biophys. J.* **2001**, *80*, 1417–28.
 (16) Veatch, S. L.; Keller, S. L. *Biophys. J.* **2003**, *84*, 725–726.
 (17) Kuzmin, P. I.; Akimov, S. A.; Chizmadzhev, Y. A.; Zimmerberg, J.; Cohen, F. S. *Biophys. J.* **2005**, *88*, 1120–1133.
 (18) Benvegnu, D. J.; McConnell, H. M. *J. Phys. Chem.* **1993**, *97*, 6686–6691.
 (19) Lancelot, E.; Grauby-Heywang, C. *Colloids Surf. B, Biointerfaces* **2007**, *59*, 81–86.
 (20) Bianco, I. D.; Maggio, B. *Colloids Surf.* **1989**, *40*, 249–260.
 (21) Ali, S.; Brockman, H. L.; Brown, R. E. *Biochemistry* **1991**, *30*, 11198–11205.
 (22) Mohwald, H. Phospholipids Monolayers. In *Structure and dynamics of membranes*; Lipowsky, R., Sackmann, E., Eds.; Elsevier: Amsterdam, 1995; pp 161–211.
 (23) Lheveder, C.; Meunier, J.; Henon, S. Brewster Angle Microscopy. In *Physical Chemistry of Biological Interfaces*; Baszkin, A., Norde, W., Eds.; Marcel Dekker, Inc: New York, 2000.
 (24) Davies, J. T.; Rideal, E. K. *Interfacial Phenomena*; Academic Press: New York, 1963.
 (25) Radhakrishnan, A.; Li, X. M.; Brown, R. E.; McConnell, H. M. *Biochim. Biophys. Acta* **2001**, *1511*, 1–6.
 (26) Hac-Wydro, K.; Wydro, P.; Dynarowicz-Latka, P.; Paluch, M. *J. Colloid Interface Sci.* **2009**, *329*, 265–272.
 (27) Honerkamp-Smith, A. R.; Veatch, S. L.; Keller, S. L. *Biochim. Biophys. Acta* **2009**, *1788*, 53–63.
 (28) Honerkamp-Smith, A. R.; Cicuta, P.; Collins, M. D.; Veatch, S. L.; den Nijs, M.; Schick, M.; Keller, S. L. *Biophys. J.* **2008**, *95*, 236–246.
 (29) Keller, S. L.; Anderson, T. G.; McConnell, H. M. *Biophys. J.* **2000**, *79*, 2033–2042.
 (30) McConnell, H. M. *Annu. Rev. Phys. Chem.* **1991**, *42*, 171–195.
 (31) Mouritsen, O. G.; Bloom, M. *Annu. Rev. Biophys. Biomol. Struct.* **1993**, *22*, 145–171.
 (32) Dumas, F.; Lebrun, M. C.; Tocanne, J. F. *FEBS Lett.* **1999**, *458*, 271–277.
 (33) Lehtonen, J. Y.; Holopainen, J. M.; Kinnunen, P. K. *Biophys. J.* **1996**, *70*, 1753–1760.
 (34) Benvegnu, D. J.; McConnell, H. M. *J. Phys. Chem.* **1992**, *96*, 6820–6824.
 (35) Esposito, C.; Tian, A.; Melamed, S.; Johnson, C.; Tee, S. Y.; Baumgart, T. *Biophys. J.* **2007**, *93*, 3169–3181.
 (36) Slotte, J. P. *Biochim. Biophys. Acta* **1995**, *1235*, 419–427.
 (37) Wurlitzer, S.; Fischer, Th. M. *J. Chem. Phys.* **2000**, *112*, 5915–5918.
 (38) Garcia-Saez, A. J.; Chiantia, S.; Schwille, P. *J. Biol. Chem.* **2007**, *282*, 33537–33544.
 (39) Veatch, S. L.; Keller, S. L. *Biophys. J.* **2003**, *85*, 3074–3083.
 (40) Marsh, D. *Biochim. Biophys. Acta* **1996**, *1286*, 183–223.
 (41) Risselada, H. J.; Marrink, S. J. *Proc. Natl. Acad. Sci. U.S.A.* **2008**, *105*, 17367–17372.